P1.8 OBSERVED RELATIONSHIPS AMONG NARROW BIPOLAR EVENTS, TOTAL LIGHTNING AND CONVECTIVE STRENGTH IN SUMMER 2005 GREAT PLAINS THUNDERSTORMS

Kyle C. Wiens*, David M. Suszcynsky
Los Alamos National Laboratory, Los Alamos, New Mexico

1. INTRODUCTION

Satellite-based Very High Frequency (VHF) lightning sensors are limited in sensitivity to a particular (but particularly powerful) intra-cloud (IC) lightning pulse [e.g., Smith et al., 1999; Jacobson, 2003; Jacobson and Light, 2003]. These powerful VHF pulses observed by satellite are often accompanied by Narrow Bipolar Events (NBEs), which are distinctive narrow electric field changes (or sferics) that have been routinely observed by ground-based VLF sensors such as the Los Alamos Sferic Array (LASA: Smith et al., 2002). The NBEs are thought to be the VLF manifestations of the powerful VHF pulses observed from orbit.

Since NBEs and their associated VHF emissions constitute the vast majority of lightning observed from orbit, the viability of global thunderstorm tracking by satellite-based VHF lightning sensors depends largely on whether NBEs can be used as robust and generic indicators of total lightning activity and convective strength. Specifically, the following questions need to be addressed:

- How do NBE rates correspond to total lightning event rates?
- Does the relationship between NBE rates and total lightning event rates depend on convective strength?

In other words, what is the meteorological setting of NBEs? Do NBEs occur in all thunderstorms, or are they more prevalent in some subset of thunderstorms–namely, severe thunderstorms?

Several recent studies have attempted to answer these questions by comparing NBE activity to various proxies of convective strength. For example, Suszcynsky and Heavner (2003) chose cloud-to-ground (CG) flash rate as their proxy. This is strictly not a valid assumption since several studies have shown that CG flash rates may decrease while total (IC plus CG) lightning flash rates increase [e.g., Williams et al., 1999; Lang and Rutledge, 2002; Wiens et al., 2005]. Nevertheless, based on observations from the LASA in Florida during the summers of 2001–2002, Suszcynsky and Heavner (2003) found a statistical correlation between NBE flash rates and CG flash rates. Jacobson and Heavner (2005) also used the lightning observations from the LASA in Florida and found that, in general, storms that produce NBEs also produce non-NBE lightning. In comparison with satellite infra-red cloud top temperatures, they found that both NBE and non-NBE lightning are selective of storms with cold cloud tops (-50 to -60°C), with essentially no lightning when cloud tops are warmer than -40°C. These collective results suggest that, like lightning in general, NBE flash rates are also correlated to the strength of thunderstorm convection.

On the other hand, there is circumstantial evidence that NBEs occur only (or are at least more prevalent) in the strongest convective storms. In the same study cited above, Suszcynsky and Heavner (2003) found many cases with non-zero CG flash rate but zero NBE rate, but these were largely limited to cases with very low CG flash rate. Assuming that CG flash rate is a proxy for convective intensity, this implies that the non-NBE cases were associated with weaker convection. Furthermore, they found that the emission heights of NBEs increased with increased NBE flash rate. Finally, Jacobson (2003) used observations from the FORTE satellite to show that the effective radiated power (ERP) of lightning events at radio frequencies (RF) is correlated with the height of the emissions. He concluded that RF-powerful IC discharges (e.g., NBEs) are heavily selective for the deepest convection.

Here, we extend these earlier studies, using an updated LASA in the Great Plains which covers a much larger geographical area (see Fig. 1) and has improved detection efficiency of IC flashes. Instead of using CG flash rate or IR cloud-top temperature as proxies for convective strength, we use observations that are more directly related to the strength of thunderstorm convection and thunderstorm severity: maximum radar reflectivity and radar echo heights.

**Corresponding author address*: Kyle C. Wiens, Los Alamos National Laboratory, ISR-2, Space and Remote Sensing Sciences Group, Los Alamos, NM 87545; email: kwiens@lanl.gov

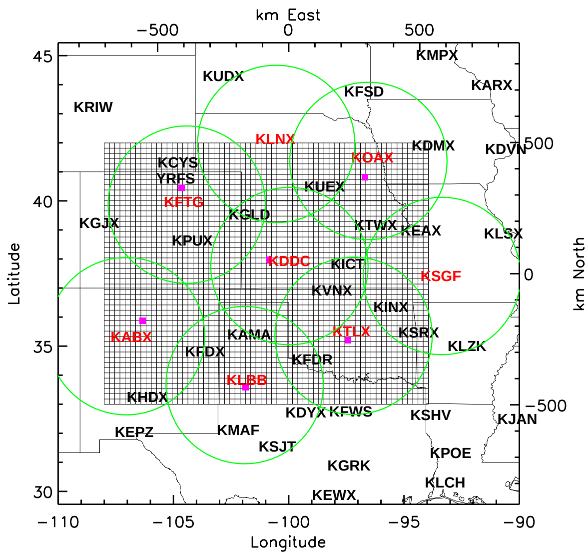

Figure 1. Computation domain used in this study. The grid extends from (-108 to -94° East) and (33 to 42° North), with 20X20 km grid resolution. NEXRAD sites are indicated with 4-letter site designations. Green rings show 300 km ranges centered on each of the eight radars (indicated by red text) used for this study. Magenta squares show the location of the six Great Plains LASA stations.

2. DATA AND METHODOLOGY

As shown in Fig. 1, the computation grid for this study is composed of 20×20 km grid cells extending from 33 to 42° North and –108 to –94° East. This domain was chosen to lie within the Great Plains LASA network in order to maximize the detection efficiency and location accuracy of lightning events. As described below, radar quantities and lightning event rates were computed and stored in 10-minute intervals for each grid cell of this domain for the entire month of June 2005.

Table 1. NEXRAD radars used in this study. All data were obtained from the NCDC website:*http://hurricane.ncdc.noaa.gov/pls/plhas/has.dsselect*.

Site name	Location
KABX	Albuquerque, NM
KDDC	Dodge City, KS
KFTG	Denver, CO
KLBB	Lubbock, TX
KLNX	North Platte, NE
KOAX	Omaha, NE
KSGF	Springfield, MO
KTLX	Oklahoma City, OK

a. Radar

It is widely recognized that the thunderstorm updraft drives the formation and growth of ice-phase precipitation, and collisions involving this ice-phase precipitation drives the electrification process (see, e.g., the review by Williams 2001). Observations have shown that total lightning flash rates increase exponentially with storm height [e.g., Ushio et al., 2001], and is also very strongly correlated with the volume of 30-40 dBZ reflectivity in the mixed phase region [e.g., Larson and Stansbury, 1974; Carey and Rutledge, 1996; MacGorman et al., 1989, Wiens et al., 2005]. Thus, in lieu of direct measurements of updraft strength and extent, radar measurements of maximum reflectivity and echo heights should provide the best routinely measured metrics of convective strength and thunderstorm severity. We make use of the nationwide coverage of the NEXRAD radar network to provide these metrics for our study.

Table 1 gives the site designation and location of the 8 NEXRAD radars used in this study. These radars are indicated by the red text in Fig. 1. For each radar volume scan, data within a range of 300 km of each radar (green circles in Fig. 1) were first interpolated onto a $4 \times 4 \times 0.5$ km Cartesian grid using NCAR's SPRINT and CEDRIC routines. The maximum reflectivity in each gridded vertical column along with the maximum altitude of 30, 40, and 50 dBZ were then extracted, thus reducing the data from each radar to only the maximum reflectivity and maximum altitude of 30, 40, and 50 dBZ in each 4X4 km horizontal grid cell. The data were then used to populate the larger (20X20 km X 10 min) computational grid by first finding the closest radar (in both space and time) to each space-time cell, then taking the largest of the 4X4 km gridded radar values that fall within the 20X20 km X 10 min grid cell. The end result is a 3-dimensional (lat X lon X time) grid which holds the maximum reflectivity and maximum altitude of 30, 40, and 50 dBZ for all time and space within the computational domain.

b. Lightning

The Great Plains Los Alamos Sferic Array (LASA) consists of six antennas stationed across the western Great Plains (indicated by the magenta squares in Fig. 1). The Great Plains LASA was deployed in April 2005. The LASA antennas record low-frequency to very-low-frequency (LF/VLF) electric field changes (or sferics) produced by lightning. When three or more stations record a lightning event, the source location of the event is determined by differential-time-of-arrival. Furthermore, an automated waveform classification routine similar to that described in Smith et al. (2002) is applied to each sferic in an attempt to identify the type of lightning (CG, IC, or NBE) that produced the sferic. The geolocated and classified lightning events were then binned into the same 3-dimensional (lat X lon X time) grid as the radar data so that the lightning events could be compared with the radar quantities at each space-time cell.

3. RESULTS

How do NBE rates relate to total lightning event rates? Figure 2a addresses this question by plotting NBE rates versus non-NBE rates for the 16,288 space-time cells during the month of June 2005 that had a non-zero NBE rate. The red and green dots show the mean and median NBE rates in space-time cells with a given non-NBE rate. Figure 2b plots the 2D histogram of the number of space-time cells with a given NBE rate versus a given non-NBE rate. There is very little indication of a correlation between NBEs and non-NBEs in either method of presentation of these data. The mean NBE rate (red dots in Fig. 2a) shows essentially no correlation with non-NBE rate until the non-NBE rate reaches >20 min^{-1}, and even then the correlation is weak. Space-time cells with large NBE rates tend to occur when non-NBE rates are small, and vice versa (Fig. 2b). These results are in stark contrast to those reported by Suszcynsky and Heavner (2003). Using the LASA in Florida, they found a much stronger correlation between NBE rates and non-NBE rates.

How are total and NBE rates related to convective strength? Figure 3a plots total LASA event rate versus maximum radar reflectivity for each of the 216,079 space-time grid cells that had both non-zero LASA event rate and maximum reflectivity >0 dBZ. Though there is considerable scatter, total LASA event rates increase with increasing maximum reflectivity. This relationship is more pronounced when the data are plotted as the mean and median LASA event rates for all space-time cells having a given maximum dBZ. That is, space-time cells with maximum dBZ within each 2.5 dBZ bin (e.g., 20 to 22.5 dBZ) were extracted, and the mean and median LASA event rates rates in these extracted cells were computed. The red and green dots in Fig. 2a show the mean and median LASA event rates for each 2.5 dBZ bin, respectively. Between 30 and 60 dBZ, the total LASA event rates increase exponentially. However, below 30 dBZ and above 60 dBZ, the total LASA event rates show little relationship to maximum dBZ. Figure 3b plots the LASA NBE rate versus maximum reflectivity for each of the 16,590 space-time grid cells that had both non-zero NBE rate and maximum reflectivity >0 dBZ. The relationship between NBEs and maximum reflectivity is not as robust as for total LASA events and maximum reflectivity; however, in the mean, the NBE rate increases exponentially between 45 and 65 dBZ, with NBE rates of 10s min^{-1} restricted to this range.

Ice and mixed-phase conditions are crucial for thunderstorm electrification, and a deeper mixed phase region implies a stronger updraft and more vigorous collisional charging processes. The freezing level for the Great Plains in the summer is near 5 km MSL, so maximum altitudes of 30 dBZ above 5 km should be a measure of the mixed-phase depth of the cloud. As shown in Fig. 4a, the total LASA event rates show a strong correlation with maximum altitude of 30 dBZ echo. Though again there is considerable scatter, from 5 to 17.5 km, the mean total LASA event rates (red dots in Fig. 4a) are proportional to the third power of 30 dBZ altitude. The LASA NBE rates also show a correlation with 30 dBZ altitude (Fig. 4b), though not as strong as for total events. Furthermore, the NBE rates show little relationship to 30 dBZ altitude for altitudes below 8 km. NBE rates of 10s min^{-1} are restricted to space-time cells with 30 dbZ altitudes above 12 km.

Figure 5 shows 2D histograms of the number of space-time cells with a given LASA event rate and a given maximum dBZ, while Figure 6 shows 2D histograms of LASA event rate and 30 dBZ altitude. Modest total LASA event rates (<10 min^{-1}) occur frequently over a wide range of maximum dBZ and 30 dBZ altitude (Figs. 5a and 6a); however, the larger total event rates are restricted to space-time cells with maximum reflectivity >35 dBZ and 30 dBZ altitudes >5 km. Modest (<1 min^{-1}) NBE event rates also occur over a wide range of the radar quantities (Figs. 5b and 6b); however, the bulk of space-time cells containing non-zero NBE rates are more restricted to reflectivity in the range of 40-60 dBZ and 30 dBZ altitudes >8 km. The few cases of NBE rates >10 min-1 occurred in space-time cells with 30 dBZ altitudes > 12 km.

Taken as a whole, these results show that total LASA events increase with increased convective strength and storm severity. The NBEs also show this relationship, but there is some indication that NBEs are more prevalent in the strongest convection. As a further illustration of this latter point, Fig. 7 shows the time series of total LASA events over the entire computation domain, for the month of June 2005. Here the total LASA events are binned into the number of events in each hour. The red curve in Fig. 7 shows the percentage of the total LASA events that were classified as NBEs. Over the whole month, the NBEs constitute 1% of total events and mean percentage of NBEs for any given hour is also 1%. However, there were a few instances where the NBEs constituted a much larger percentage of the total. The most spectacular example of large percent-NBEs occurred in a pair of severe storms on 27-28 June. A brief overview of this case is presented next.

a. NBE storm on 27-28 June

Figure 8 shows swaths of maximum reflectivity produced by a pair of storms in eastern Nebraska. The upper panel shows the radar observations from the KCYS radar in Cheyenne from 1940–2400 UTC on 27 June. The lower panel shows the radar observations of just the southern storm from the KLNX radar in North Platte from 0000–0500 on 28 June. Both of these storms were severe, with numerous large hail reports associated with both storms. (These are *preliminary* severe reports that have not yet been validated.) The southern storm had all the hallmarks of a supercell: It took a right turn and developed southward of the mean eastward progression of other storms on this day. It was associated with several *preliminary* tornado reports. It had a sustained and pronounced bounded weak echo region on its right flank (not shown).

Figure 9 shows the same maximum reflectivity swaths as Fig. 8, but in gray-scale and with LASA events overlaid and color-coded by event type. Both the northern and southern storms produced large quantities of NBEs. The northern storm produced only positive polarity NBEs over only a short duration. The southern storm produced large quantities of NBEs, of both polarities, for several hours, with little other lightning activity (note the event totals in the legends of Fig. 9). Note also the lack of NBEs, and prevalence of CG events, in the weaker convection surrounding these two storms. Hence, in these two storms, the NBEs were more prevalent in the stronger, more severe convection and largely absent from weaker convection. A more detailed analysis of these two storms in currently underway.

4. Summary and Discussion

In this study, we compared lightning event rates measured by LASA to NEXRAD radar-based metrics of convective strength for the month of June 2005 in the Great Plains. Based on this comparison, we have the following observations based largely on statistical analysis of gridded quantities.

1. Total LASA event rates increase exponentially with both increased maximum reflectivity (Fig. 3a) and increased altitude of 30 dBZ (Fig. 4a), with total LASA event rate proportional to the third power of 30 dBZ height for altitudes above the freezing level.

2. LASA NBE rates also increase with both increased maximum reflectivity (Fig. 3b) and 30 dBZ height (Fig. 4b), but these relationships for NBEs are not as robust as they are for total LASA rates.

3. There is little apparent correlation between NBEs and total LASA events (Fig. 2). Space-time cells with larger NBE rates tend to occur in space-time cells with smaller total event rates, and vice versa.

4. NBEs seem to be more prevalent in the strongest convection. Space-time cells with elevated NBE rates tend to have maximum reflectivity in the range of 40-60 dBZ (Fig. 5b) and 30 dBZ heights >8 km (Fig. 6b).

5. NBEs constitute 1% of all lightning events observed by LASA; however, in some storms, NBEs make up a much larger percentage. In the case of the severe storms on 27-28 June, the NBEs constituted as much as 60% of the total LASA events.

Since these June 2005 results indicate that NBEs are more prevalent in the strongest storms, our future analysis will focus on determining whether this correlation between NBEs and severe storms goes both ways. That is, do all severe storms produce frequent NBEs? Or is it just that NBE-producing storms also happen to be severe? The answer to this question will no doubt require a larger statistical sample. We will thus extend our statistical analysis to the remaining summer months of 2005 and conduct more detailed analysis of several individual storms.

References

Carey, L. D. and S. A. Rutledge, 1996: A multiparameter radar case study of the microphysical and kinematic evolution of a lightning producing storm. *Meteorol. Atmos. Phys.*, **59**, 33–64.

Jacobson, A. R., 2003: Relationship of intracloud-lightning radio frequency power to lightning-storm height, as observed by the FORTE satellite. *J. Geophys. Res.*, **108**, doi:1029/2002JD002956.

Jacobson, A. R. and M. J. Heavner, 2005: Comparison of narrow biplolar events with ordinary lightning as proxies for severe convection. *Mon. Wea. Rev.*, **133**, 1144–1154.

Jacobson, A. R. and T. Light, 2003: Bimodal radio frequency pulse distribution of intracloud-lightning signals recorded by the FORTE satellite. *J. Geophys. Res.*, **108**, doi:1029/2002JD002613.

Lang, T. J. and S. A. Rutledge, 2002: Relationships between convective storm kinematics, precipitation, and lightning. *Mon. Wea. Rev.*, **130**, 2492–2506.

Larson, H. R. and E. J. Stansbury, 1974: Association of lightning flashes with precipitation cores extending to height 7 km. *J. Atmos. Terr. Phys.*, **36**, 1547–1553.

MacGorman, D. R., D. W. Burgess, V. Mazur, W. D. Rust, W. L. Taylor, and B. C. Johnson, 1989: Lightning rates relative to tornadic storm evolution on 22 May 1981. *J. Atmos. Sci.*, **46**, 221–250.

Smith, D. A., K. B. Eack, J. Harlin, M. J. Heavner, A. R. Jacobson, R. S. Massey, X. M. Shao, and K. C. Wiens, 2002: The Los Alamos Sferic Array: A research tool for lightning investigations. *J. Geophys. Res.*, **107**.

Smith, D. A., X. M. Shao, D. N. Holden, C. T. Rhodes, M. Brook, P. R. Krehbiel, M. Stanley, W. Rison, and R. J. Thomas, 1999: A distinct class of isolated intracloud lightning discharges and their associated radio emissions. *J. Geophys. Res.*, **104**, 4189–4212.

Suszcynsky, D. M. and M. J. Heavner, 2003: Narrow bipolar events as indicators of convective strength. *Geophys. Res. Lett.*, **30**, doi:10.1029/2003GL017834.

Ushio, T., S. J. Heckman, D. J. Boccippio, H. J. Christian, and Z. I. Kawasaki, 2001: A survey of thunderstorm flash rates compared to cloud top height using TRMM satellite data. *J. Geophys. Res.*, **106**, 24,089–24,095.

Wiens, K. C., 2005: *Kinematic, Microphysical, and Electrical Structure and Evolution of Thunderstorms during the Severe Thunderstorm Electrification and Precipitation Study (STEPS)*. Ph.D. thesis, Colorado State University, Fort Collins, 295 pp.

Williams, E. R., 2001: The electrification of severe storms. *Severe Convective Storms*, C. A. D. III, ed., Amer. Meteor. Soc., volume 50 of *Meteor. Monogr.*, 527–561.

Williams, E. R., B. Boldi, A. Matlin, M. Weber, S. Hodanish, D. Sharp, S. Goodman, R. Raghaven, and D. Buechler, 1999: The behavior of total lightning activity in severe Florida thunderstorms. *Atmos. Res.*, **51**, 245–264.

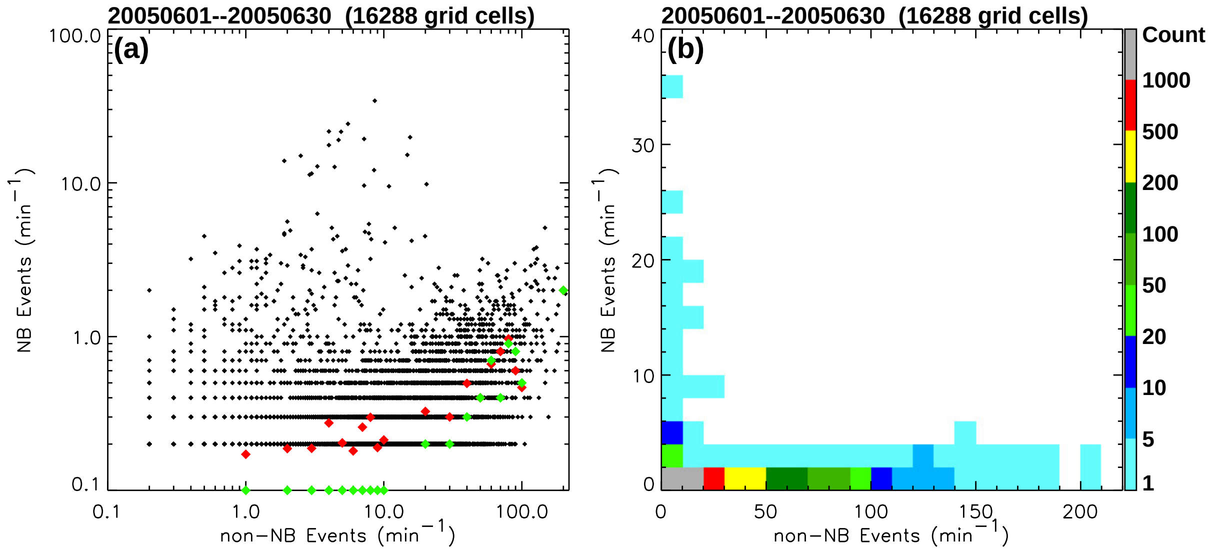

Figure 2. (a) LASA NBE rate versus LASA non-NBE event rate (black dots) with the mean and median NBE rate for a given non-NBE event rate indicated by the red and green dots, respectively. (b) 2D histogram of the number of space-time cells with a given non-zero NB event rate and a given non-zero non-NB event rate.

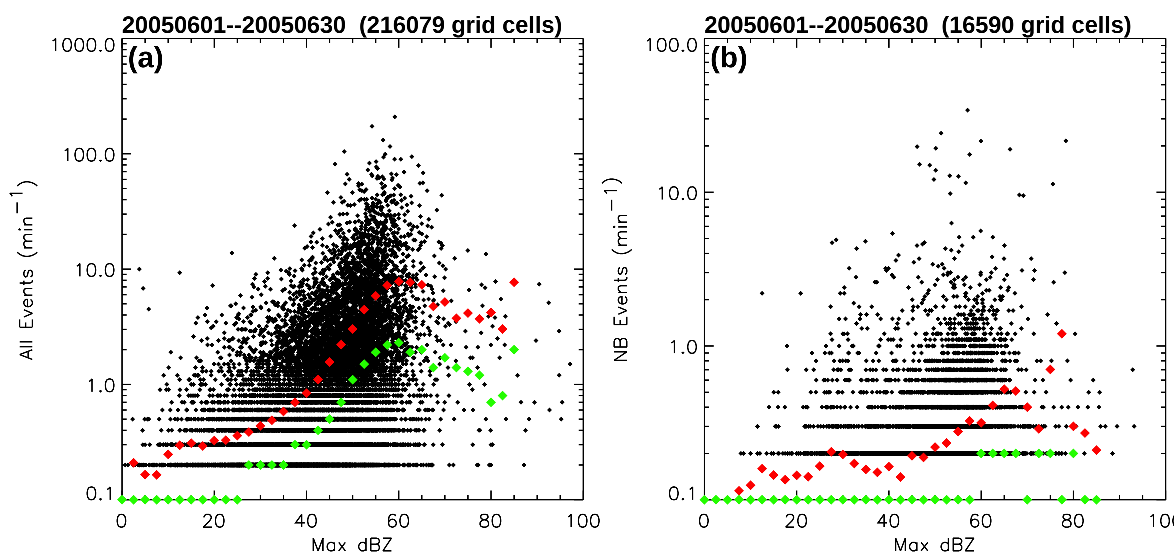

Figure 3. LASA event rates versus maximum radar reflectivity for (a) all events and (b) NB events. Black dots show all space-time cells having both non-zero LASA event rates and reflectivity >0 dBZ. Red (green) dots show the mean (median) LASA event rates in space-time cells having a given maximum reflectivity in bins of 2.5 dBZ.

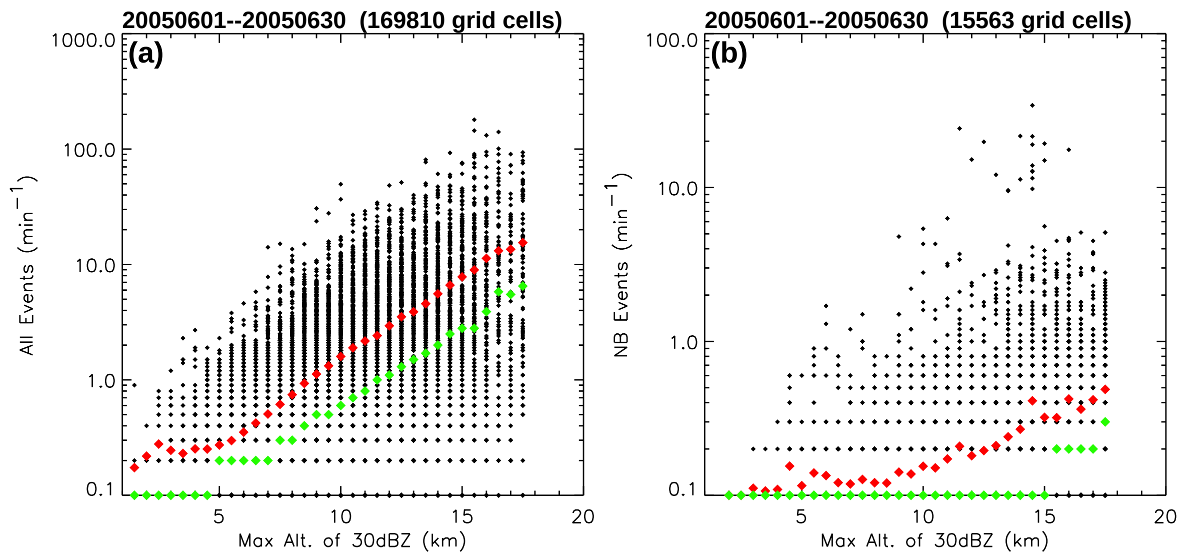

Figure 4. As in Fig. 3, but with LASA events versus max altitude of 30 dBZ. Altitude bins are 0.5 km.

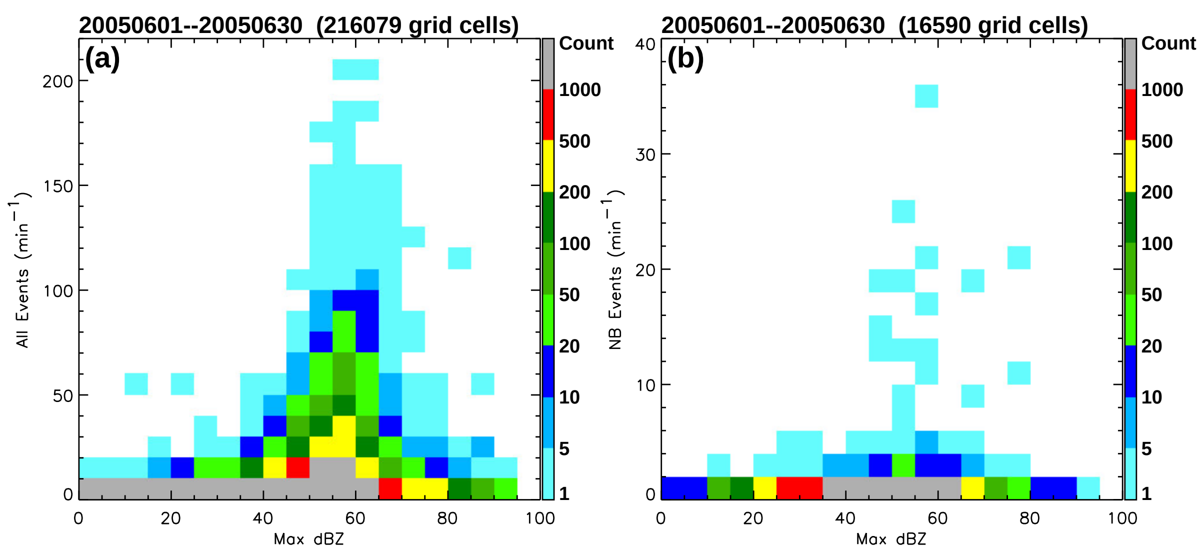

Figure 5. 2D histograms of the number of space-time cells with (a) a given non-zero LASA total event rate and a given maximum reflectivity and (b) a given non-zero LASA NB event rate and a given maximum reflectivity.

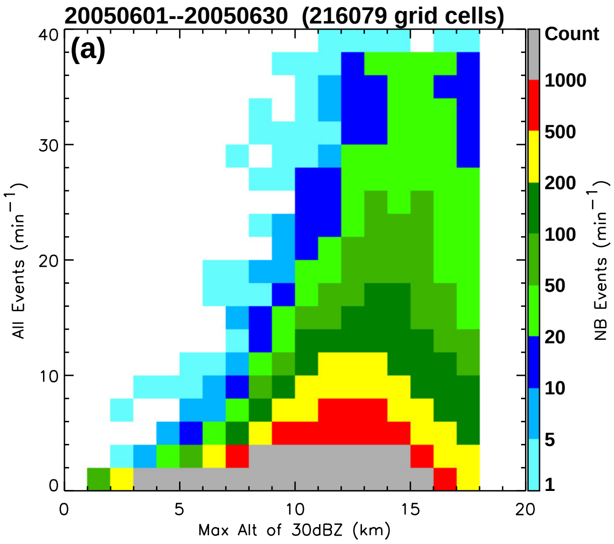

Figure 6. As in Fig. 5, but for LASA event rates and maximum altitude of 30 dBZ.

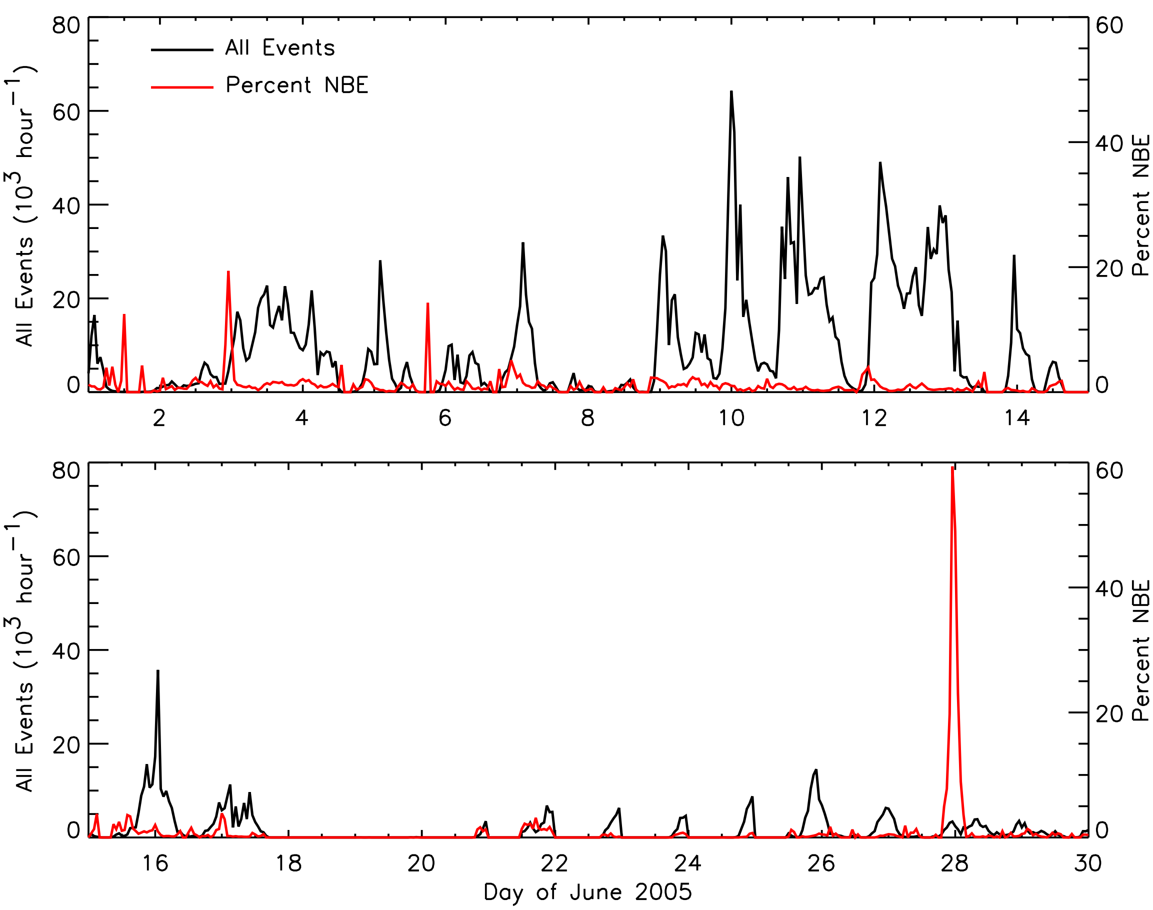

Figure 7. Time series of total LASA event counts in each UTC hour within the entire computation domain (black curve), with hourly percentage of NBEs (red curve). NBEs constitute 1% of the total.

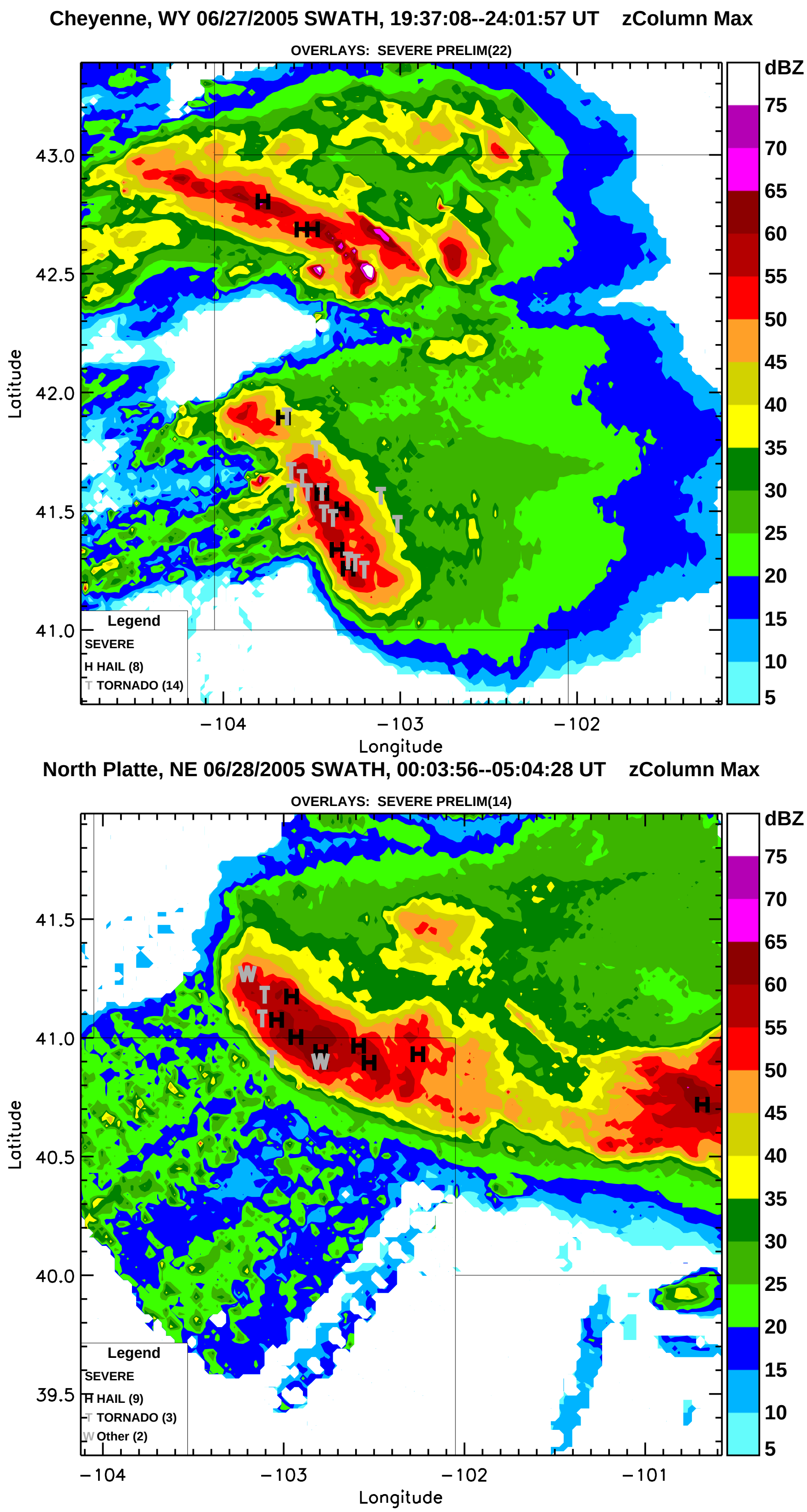

Figure 8. Swath of maximum reflectivity with preliminary severe storm reports: (top) KCYS radar from 1940 to 0000 UTC on 27 June. (bottom) KLNX radar from 0000 to 0500 UTC on 28 June. Storm motion is to the southeast.

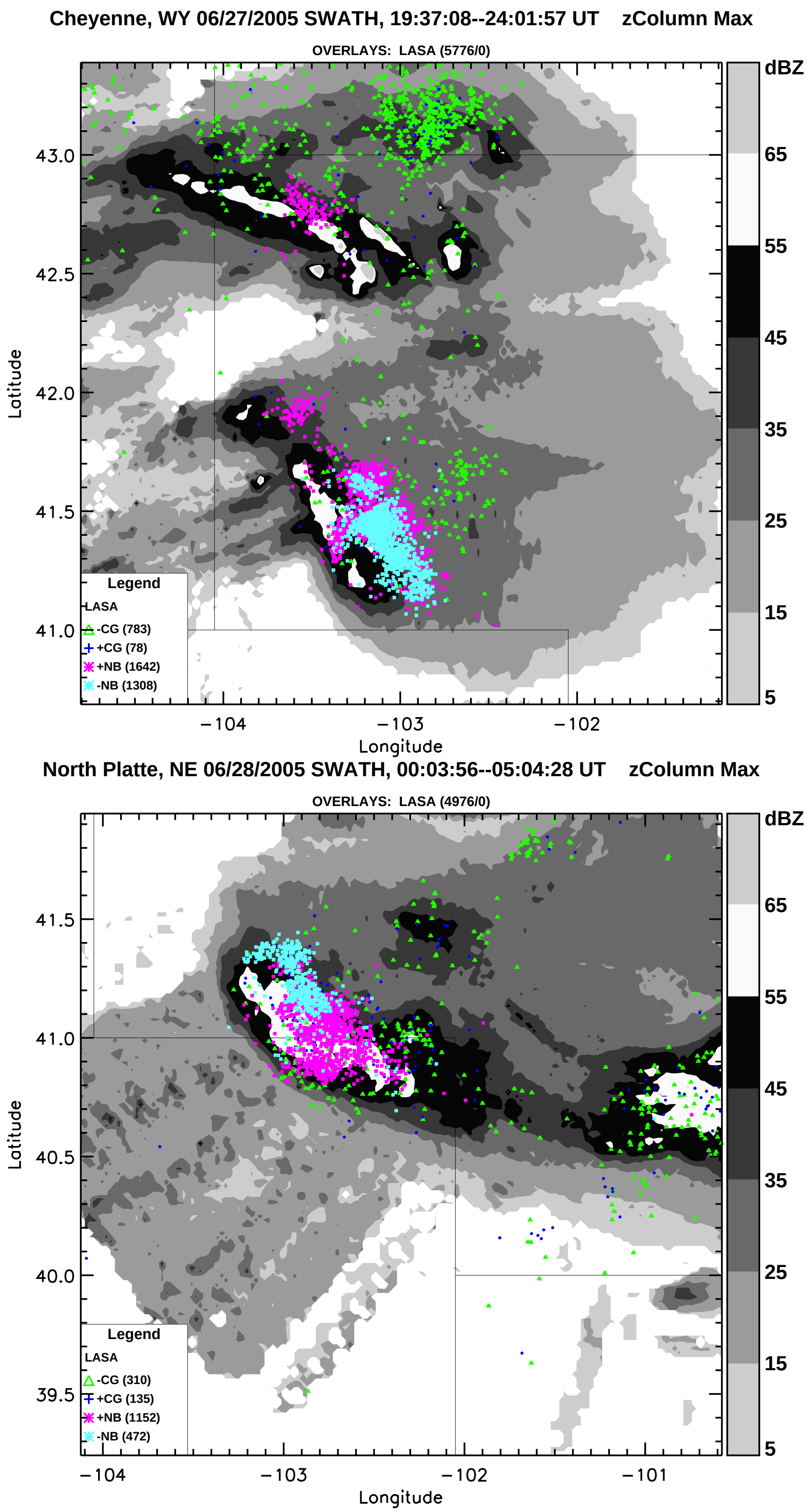

Figure 9. As in Fig. 8, but with max reflectivity in gray-scale and with overlaid LASA events color-coded by event type. For clarity, generic IC events are not shown.